Study and Implementation of IEEE 802.11p PHY for OFDM Underwater Acoustic Communications

Xilin Cheng and Liuqing Yang
Department of Electrical and Computer Engineering
Colorado State University

***Abstract*—Underwater acoustic sensor networks (UWASNs) have been attracting growing interests from academia and industry in recent decades due to the emerging applications. However, their standardization is still in the stage of exploration. This work investigates the possible standardization of orthogonal frequency-division multiplexing (OFDM) underwater acoustic communications (UAC). Due to the similarities between vehicular channels and underwater acoustic (UWA) channels such as the multipath wave propagation and the Doppler shift, the industrial IEEE 802.11p which contains the physical layer (PHY) specifications for OFDM communications in vehicular environments can serve as a valuable reference. In this work, we study and implement IEEE 802.11p PHY for OFDM UAC. An OFDM UAC simulator is built based on IEEE 802.11p PHY with the system parameters modified according to the UWA channel features. The performance of three channel estimators, namely the least square (LS) estimator, the spectral temporal averaging (STA) estimator and the symbol-wise (SW) estimator is evaluated. It is found that the SW estimator outperforms the LS estimator and the STA estimator which are commonly used for IEEE 802.11p PHY. This is because the SW estimator is more capable of tracking the fast time-varying UWA channels. Finally, the extension of OFDM UAC to the multiple-input and multiple-output (MIMO) system is discussed.**

I. Introduction

Underwater acoustic sensor networks (UWASNs) have been attracting growing interests from academia and industry in recent decades due to the emerging applications including marine resource exploration, remote control in off-shore oil fields, pollution monitoring, ocean observation, and military purposes [1], [2]. However, compared with terrestrial networks, their standardization is still in the stage of exploration [3], [4]. Nevertheless, considering the fast development of sensor and communication technologies as well as the benefits of standardization towards underwater networking research, product development and commercialization, the standardization progress could be boosted in the near future.

An important part of standardization is the physical layer (PHY) implementation of UWASNs to enable interoperability between modems from different vendors. There exists a few standards of underwater acoustic communications (UAC). For example, Woods Hole Oceanographic Institution (WHOI) defines a PHY standard based on frequency shift keying with frequency hopping (FH-FSK) with data rate up to 80 bps [5], and the standard is supported by the WHOI micro modem and the modems from Teledyne Benthos [6]. Recently, orthogonal frequency-division multiplexing (OFDM) communications has attracted great interests because of its high data rate, capability of intersymbol interference (ISI) removal and robustness against large delay spread [7], [8]. Therefore, it is a promising candidate of communication techniques for the future UAC standardization.

To standardize OFDM UAC, the industry standard IEEE 802.11p [9] which contains PHY specifications for OFDM communications in vehicular environments can serve as a valuable reference due to the similarities between vehicular channels and underwater acoustic (UWA) channels. First, both of them feature multipath wave propagation that causes frequency selective fading and ISI. Secondly, for both channels, there exists the Doppler shift resulting from motion. To cope with these channel features, IEEE 802.11p PHY adopts OFDM to combat ISI and the preamble for signal detection, time synchronization, carrier frequency offset (CFO) compensation and channel estimation. However, IEEE 802.11p PHY can not be directly applied to OFDM UAC because of its particular channel features such as low carrier frequency and bandwidth, large delay spread, severe Doppler shift, and fast time-varying channel response. Corresponding modifications have to be made for OFDM UAC.

This work focuses on the implementation and performance evaluation of IEEE 802.11p PHY for OFDM UAC. We build an OFDM UAC simulator based on IEEE 802.11p PHY with system parameters modified according to the particular features of UWA channels. The performance of two channel estimators commonly used for IEEE 802.11p, namely the least square (LS) estimator and the spectral temporal averaging (STA) estimator, is evaluated. The simulation results show that the LS estimator and the STA estimator have poor bit error rate (BER) performance, which implies that they fail to track the fast time-varying UWA channels. Therefore, we consider the symbol-wise (SW) estimator for OFDM UAC, where each OFDM symbol estimates its own channel frequency response (CFR). The simulation results confirm that the SW estimator outperforms the LS estimator and the STA estimator. Finally, OFDM UAC is extended to the multiple-input and multiple-output (MIMO) system with higher data rate and reliability.

The rest of the paper is organized as follows. In Section II, the frame structure and the channel estimators of IEEE 802.11p PHY are introduced. In Section III, the modifications of IEEE 802.11p PHY for OFDM UAC are discussed. In Section IV, the OFDM UAC simulator is described. The performance of channel estimators and the MIMO system is also present. Summarizing remarks are given in Section V.

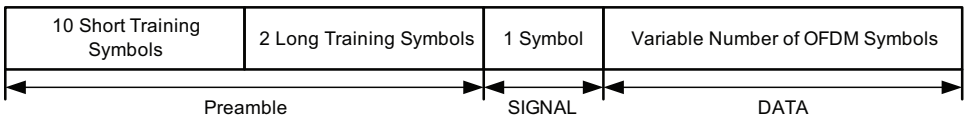

Fig. 1. Frame structure of PPDU specified by IEEE 802.11p

II. IEEE 802.11p PHY

In this section, the frame structure of IEEE 802.11p and the respective channel estimation schemes are briefly introduced.

A. IEEE 802.11p Frame Structure

The IEEE 802.11p standard is an amendment of the IEEE 802.11a standard [10]. It aims at wireless access in the vehicular environment (WAVE) in the licensed intelligent transportation system (ITS) band 5.85 - 5.925 GHz. In order to combat the multipath effect in the vehicular environment, the bandwidth utilized by IEEE 802.11p is 10 MHz, which is half of that of IEEE 802.11a. The data rates supported by IEEE 802.11p include 3, 4.5, 6, 9, 12, 18, 24, and 27 Mbps depending on different modulation and puncturing schemes.

The frame structure of the physical protocol data unit (PPDU) defined by IEEE 802.11p is shown in Fig. 1. It consists of the Preamble field, the SIGNAL field, and the DATA field. In the Preamble field, ten short training symbols are used for signal detection, coarse frequency offset estimation, and time synchronization. The two long training symbols T_1 and T_2 are used for channel and fine frequency offset estimation. The total length of the Preamble field is 32 μs. The SIGNAL field consists of one OFDM symbol conveying information about the type of modulation, the coding rate, etc. The DATA field includes the data for transmission with the number of OFDM symbols undefined. The length of each OFDM symbol is 6.4 μs. The guard interval (GI) with the length 1.6 μs is inserted before each OFDM symbol to remove ISI.

B. Channel Estimation Schemes

There are two commonly used channel estimators for IEEE 802.11p PHY, namely the LS estimator and the STA estimator.

1) LS Estimator: The LS estimator is the most commonly used channel estimation scheme [11]. Define the received signals on subcarrier k at the two long training symbols as $Y_{T_1}(k)$ and $Y_{T_2}(k)$. Then the estimated CFR is give as:

$$H(k) = \frac{Y_{T_1}(k) + Y_{T_2}(k)}{2X(k)}. \tag{1}$$

The estimated CFR is used for equalization of the subsequent OFDM symbols.

2) STA Estimator: The LS estimator is effective for relatively stationary environments. However, when employed for high-mobility environments, it is incapable of estimating the time-varying channels. To handle the time-varying feature of vehicular channels, the STA estimator is proposed [12].

The first step of the STA estimator is to perform channel estimation using the LS estimator, i.e., $H_{STA,0}(k) = H(k)$, and the estimated CFR is utilized to decode the first OFDM symbol following the preamble.

Suppose $H_{STA,i}(k)$ is the estimated CFR at the kth subcarrier of the ith OFDM symbol using the STA estimator. The received signal at the $i+1$th OFDM symbol is equalized by $H_{STA,i}(k)$:

$$\widetilde{X}_{i+1}(k) = \frac{Y_{i+1}(k)}{H_{STA,i}(k)}, \tag{2}$$

and $\widetilde{X}_{i+1}(k)$ is demapped to $\widehat{X}_{i+1}(k)$ according to the adopted modulation scheme. Then the updated channel estimation of the $i+1$th OFDM symbol is given as:

$$H_{i+1}(k) = \frac{Y_{i+1}(k)}{\widehat{X}_{i+1}(k)}. \tag{3}$$

To mitigate the detrimental effect caused by the data subcarriers incorrectly detected, averaging the estimated CFR in both the frequency domain and the time domain is necessary. The frequency domain averaging is given as:

$$H_{freq,i+1}(k) = \frac{1}{2\beta+1} \sum_{j=-\beta}^{\beta} H_{i+1}(k+j), \tag{4}$$

and the time domain averaging result is obtained as:

$$H_{STA,i+1}(k) = \left(1 - \frac{1}{\alpha}\right) H_{STA,i}(k) + \frac{1}{\alpha} H_{freq,i+1}(k). \tag{5}$$

Then $H_{STA,i+1}(k)$ is utilized to decode the $i+2$th OFDM symbol. The entire process ends when the last OFDM symbol in the packet is decoded.

III. Modifications of IEEE 802.11p PHY for OFDM UAC

Both of vehicular channels and UWA channels feature multipath wave propagation and Doppler shifting. Therefore, IEEE 802.11p PHY can serve as a valuable reference for the OFDM UAC standardization. However, because of the particular features of UWA channels, IEEE 802.11p PHY can not be directly applied, and the corresponding modifications have to be made. First, the acoustic signal is characterized by the low carrier frequency and bandwidth in the order of kHz. The low bandwidth implies the long OFDM symbol duration. For example, with the bandwidth 6 kHz and the total subcarrier number 1024, the length of an OFDM symbol is 170 ms which is much longer than the length 6.4 μs defined by IEEE 802.11p. Secondly, the very slow acoustic propagation speed ($c \approx 1500$ m/s) and the multipath nature of UWA channels result in much larger delay spread, which is around tens or even hundreds of milliseconds. This implies the length of GI for OFDM UAC is much longer than 1.6 μs defined by IEEE

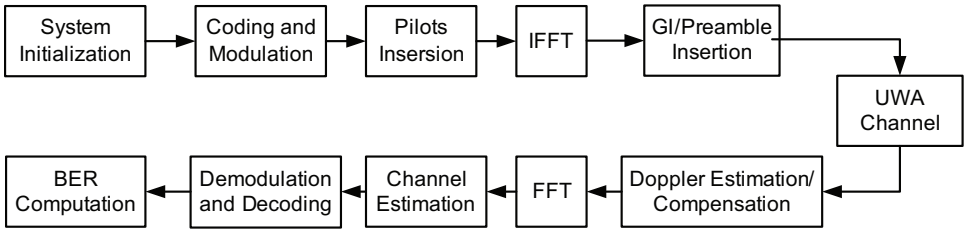

Fig. 2. System diagram of the OFDM UAC simulator

802.11p. Finally, UWA channels are fast time-varying, and UAC experiences much severer Doppler shifting compared with vehicular communications, i.e., the normalized frequency offset factor $a = v/c$ in UWA channels can be on the order of 10^{-3} compared with 10^{-7} for vehicular channels [13]. Considering the very long OFDM symbol length, OFDM symbols could experience different Doppler shifts and CFRs. Therefore, it is preferable that each OFDM symbol estimates its own Doppler shift and CFR.

Based on the above discussions, two kinds of modifications of IEEE 802.11p PHY could be made for OFDM UAC. First, the system parameters of IEEE 802.11p PHY such as OFDM symbol duration, GI duration, signal bandwidth and carrier frequency have to be modified according to the particular features of UWA channels. Secondly and more importantly, the channel estimators for UWA channels have to be carefully chosen. In Section IV, we build an OFDM UAC simulator to evaluate the performance of the LS estimator and the STA estimator. We also implement the SW estimator which is more capable of tracking the fast time-varying UWA channels.

IV. OFDM UAC Simulator Based on IEEE 802.11p PHY

In this section, we build an OFDM UAC simulator based on IEEE 802.11p PHY. The system diagram is given in Fig. 2. In the simulator, the system initialization module defines the system parameters such as bandwidth, carrier frequency, FFT size, OFDM symbol duration, GI duration, etc. The coding and modulation module implements data encoding and modulation, and the modulated data symbols are placed on the data subcarriers of OFDM symbols. In the pilots insertion module, the pilots are uniformly inserted among data subcarriers. In the GI/preamble insertion module, GI is inserted before each OFDM symbol, and the preamble is placed at the beginning of all the generated OFDM symbols. UWA channel module generates the time-varying baseband UWA channel response. In the Doppler estimation and compensation module, each received OFDM symbol estimates and compensates its own CFO. In the channel estimation module, the CFRs of OFDM symbols are estimated. In the demodulation and decoding module, based on the estimated CFRs, data symbols in each OFDM symbol are equalized and decoded. In the following, the main components of the OFDM UAC simulator are detailed.

TABLE I
System parameters

IFFT Size	1024
Carrier Frequency	17 kHz
Signal Bandwidth	6 kHz
Number of Active Subcarriers	1012
Number of Null Subcarriers	92
Number of Phase Tracking Subcarriers	68
Subcarrier Spacing	5.86 Hz
OFDM Symbol Duration	170.7 ms
GI Duration	42.67 ms

A. System Initialization

The system parameters of the OFDM UAC simulator are provided in Table I, which are designed based on the UAC channel features. The inverse fast Fourier transform (IFFT) size is chosen to be $N = 1024$, and the 1024 OFDM subcarriers include 852 active subcarriers, 92 null subcarriers, 68 phase tracking subcarriers, and 12 virtual subcarriers. For the LS estimator and the STA estimator, all 852 active subcarriers are data subcarriers. In contrast, for the SW estimator, among the 852 active subcarriers, 718 subcarriers are data subcarriers and 134 subcarriers are pilot subcarriers used for channel estimation.

B. Acoustic Channel Simulator

The acoustic channel simulator in [14], [15] is adopted in our OFDM UAC simulator to generate the time-varying channel response. The simulator takes into account both large-scale and small-scale variations as well as motion-induced Doppler effect. The following setup is adopted in the acoustic channel simulator. The water depth is 100 m. The depth of the transmitters is 80 m, and the depth of the receiver is 50 m. The distance between the transmitter and the receiver is 1000 m. For the large-scale effect, the geometric multipath structure is used to calculate path gains and delays. For the small-scale effect, the intrapath amplitude is modeled as a complex Gaussian random variable, and the intrapath delay is modeled as a first-order autoregressive process. Three types of motion influence the Doppler shift, i.e., drifting, vehicular motion, and surface motion. The maximum drifting speed of the transmitter is 0.1 m/s, and the maximum drifting speed of the receiver is 0.02 m/s. The motion speed of transmitter is around 1.1 m/s, and the motion speed of the receiver is 0 m/s. The surface waves move up and down sinusoidally in time

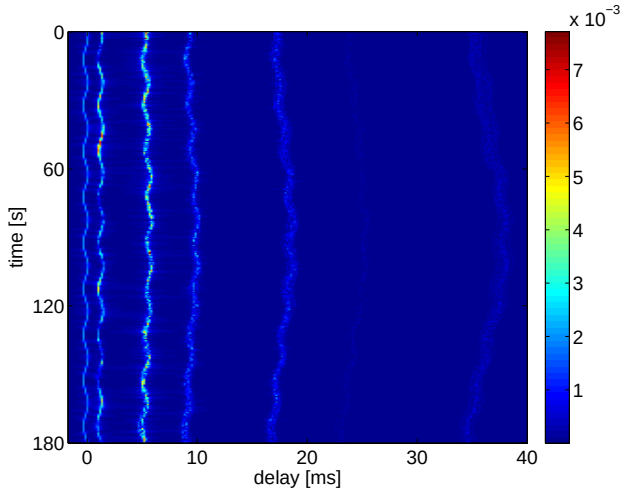

Fig. 3. The time-varying channel response generated by the acoustic channel simulator

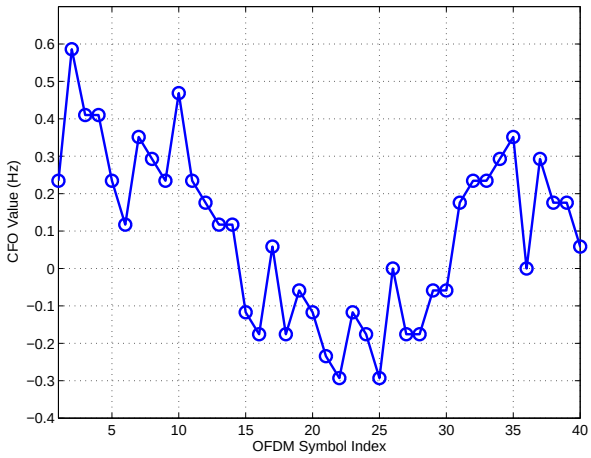

Fig. 4. Estimated CFO values

with the amplitude 0.05 m and the frequency 0.01 Hz. The generated time-varying channel response in the time domain is given in Fig. 3. The channel response is then truncated to 10 ms and convolved with the data packet.

C. Doppler Estimation and Compensation

We adopt the method in [7] to estimate and compensate CFO. Null subcarriers which are uniformly inserted over all data and pilot subcarriers are used for CFO estimation.

Suppose that the received baseband OFDM signal in the time domain is $\boldsymbol{y} = [y_0, y_1, \cdots, y_{N-1}]^T$. Give a tentative CFO value ε, CFO is compensated as:

$$\widetilde{y} = \boldsymbol{D}^H(\varepsilon)\boldsymbol{y}, \tag{6}$$

where $\boldsymbol{D}(\varepsilon) = \text{diag}\left(\left[1, e^{j2\pi\varepsilon/N}, \cdots, e^{j2\pi\varepsilon(N-1)/N}\right]\right)$. Then the total energy of null subcarriers can be calculated as:

$$J(\varepsilon) = \|\boldsymbol{M}\boldsymbol{F}_N\widetilde{y}\|^2, \tag{7}$$

where $\boldsymbol{F}_N$ is the $N \times N$ discrete Fourier transform (DFT) matrix and $\boldsymbol{M}$ is the mapping matrix for null subcarriers. Then the CFO is estimated as

$$\widehat{\varepsilon} = \arg\min_{\varepsilon} J(\varepsilon). \tag{8}$$

The estimated CFO is compensated using Eq. (6).

Fig. 4 depicts the estimated CFO of 40 consecutive OFDM symbols generated by the OFDM UAC simulator. It is observed that OFDM symbols experience different Doppler shifts. This shows that CFO estimation and compensation for each OFDM symbol is preferable.

D. Channel Estimation

The LS estimator and the STA estimator have been detailed in Section II-B. Here, we focus on the SW estimator. For the SW estimator, each OFDM symbol estimates its own CFR. The CFR on the pilot subcarriers are estimated first using the estimator:

$$H(k_p) = Y(k_p)/X(k_p), \tag{9}$$

where $X(k_p)$ is the transmitted pilot symbol at the pilot subcarrier k_p and $Y(k_p)$ is the received signal. Then the CFR on the data subcarriers can be obtained through the piecewise cubic spline interpolation.

The SW estimator also brings two modifications towards the packet structure. First, more pilots are utilized for channel estimation resulting in some loss of spectral efficiency. Secondly, as each OFDM symbol is able to estimate its own CFR and Doppler shift, the two long training symbols in the preamble are not necessary.

E. Extension to the MIMO System

The MIMO technique can be applied to OFDM UAC to improve its transmission rate and reliability. Suppose that there are N_t transmitters and N_r receivers in the OFDM UAC system. Let $\boldsymbol{y}_k$ and $\boldsymbol{x}_k$ be the receive and transmit vectors at the data subcarrier k. Then $\boldsymbol{y}_k$ and $\boldsymbol{x}_k$ have the following relationship:

$$\boldsymbol{y}_k = \boldsymbol{H}_k\boldsymbol{x}_k + \boldsymbol{n}, \tag{10}$$

where $\boldsymbol{H}_k$ is the $N_r \times N_t$ channel matrix with $\boldsymbol{H}_k(i,j)$ being the CFR between the ith receiver and the jth transmitter and $\boldsymbol{n}$ is the noise vector, i.e., $\boldsymbol{n} \sim \mathcal{CN}(0, \boldsymbol{R})$ with $\boldsymbol{R} = \text{diag}\left(\left[\sigma_1^2, \sigma_2^2, \cdots, \sigma_{N_r}^2\right]\right)$. σ_i^2 is the noise and intercarrier interference (ICI) power at the receiver i, and it can be estimated by averaging the power of all null subcarriers. To estimate the channel matrix $\boldsymbol{H}_k$, we adopt the orthogonal pilot structure design as shown in Fig. 5. The pilot subcarriers from different transmitters are designed to be orthogonal with each other. Then the CFR for each transmitter-receiver pair can be directly estimated using the method in Section IV-D.

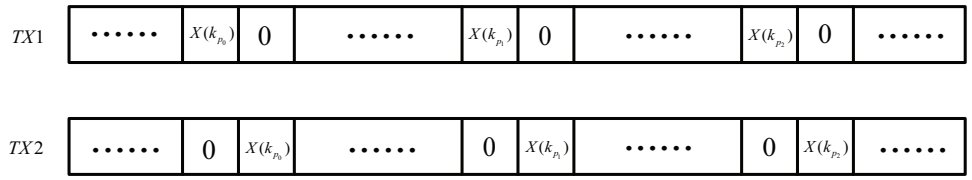

Fig. 5. Orthogonal pilot structure for the MIMO system

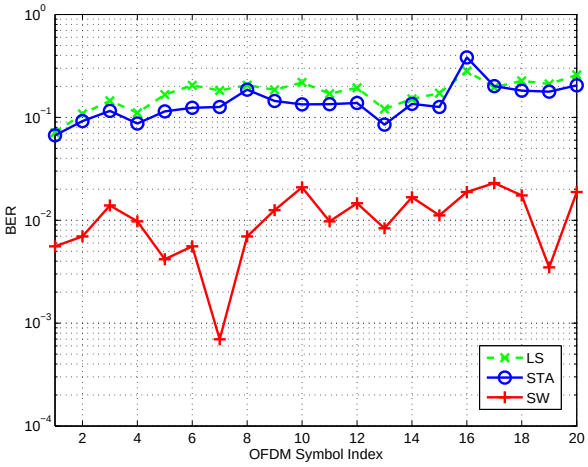

Fig. 6. Uncoded BER performance of the LS estimator, the STA estimator, and the SW estimator in the SISO OFDM UAC system

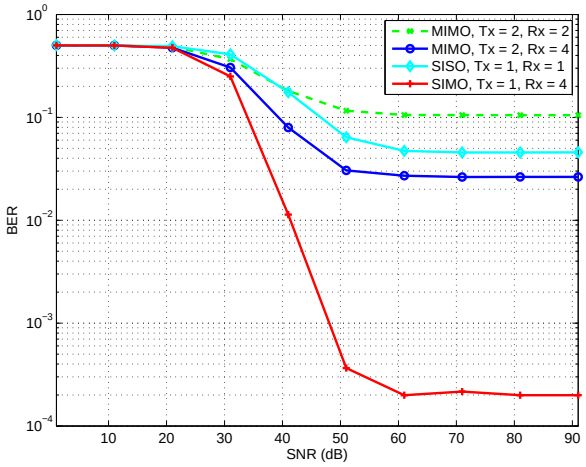

Fig. 7. Performance of the SISO system, the SIMO system, and the MIMO system using the OFDM UAC simulator

The minimum mean square error (MMSE) estimation of transmit data symbol $\boldsymbol{x}_k$ can be computed as:

$$\widehat{\boldsymbol{x}}_k = \boldsymbol{H}_k^H (\boldsymbol{H}_k \boldsymbol{H}_k^H + \boldsymbol{R})^{-1} \boldsymbol{y}_k. \tag{11}$$

Then $\widehat{\boldsymbol{x}}$ is detected according to the adopted modulation scheme. It is worth noticing that the V-BLAST algorithm can further improve the performance of the MIMO system but with the increased receiver complexity [16].

F. Performance Evaluation

In Fig. 6, the uncoded BER performance of the LS estimator, the STA estimator and the SW estimator in the single-input and single-output (SISO) OFDM UAC system is evaluated. QPSK modulation and Gray code are adopted. For the STA estimator, $\alpha = \beta = 2$. It can be observed that the SW estimator outperforms the LS estimator and the STA estimator. This is because the SW estimator is more capable of tracking the channel variations over time for OFDM UAC, compared with the LS estimator and the STA estimator.

In Fig. 7, we simulate the performance of the MIMO system using the OFDM UAC simulator. The performance of the SISO system and the single-input and multiple-output (SIMO) system is also provided. In the simulator, the SW estimator is adopted. The distance between the adjacent transmitters is 0.5 m and the distance between the adjacent receivers is 0.2 m. For the MIMO system with $N_t = 2$, the number of pilot subcarriers for channel estimation doubles, i.e., 268 according to the orthogonal pilot structure design, and the number of data subcarriers is reduced to be 584. The data rate of the MIMO system without considering the GI and the preamble is 6.8 kbps, which is still much higher than the data rate of the SISO system, i.e., 4.2 kbps. From Fig. 7, it can be observed that the MIMO system with $N_t = 2$ and $N_r = 4$ outperforms the SISO system. This confirms that the MIMO system could improve both the transmission rate and reliability. In addition, the MIMO system with $N_t = N_r = 2$ has worse performance than the SISO system. This is because for the MIMO system, the CFOs of two transmitters can not be fully compensated simultaneously. The SIMO system with $N_t = 1$ and $N_r = 4$ is most reliable as it has the highest diversity order, i.e., 4. Finally, it is worth noticing that due to ICI, which can not be fully removed by CFO compensation, the error floors exist.

V. Conclusions

This paper discusses the possible standardization and the corresponding performance evaluation of OFDM UAC with the IEEE 802.11p standard serving as the reference. Based on IEEE 802.11p PHY, we build an OFDM UAC simulator for the purpose of the performance evaluation. The parameters of IEEE 802.11p PHY such as bandwidth, OFDM symbol duration, GI duration, etc., are modified according to the UWA channels features. As OFDM symbols could experience different Doppler shifts, the Doppler shift is estimated and compensated for each OFDM symbol using null subcarriers.

The simulator implements three channel estimators, namely the LS estimator, the STA estimator and the SW estimator. It is found that the SW estimator which estimates the CFR of each OFDM symbol using pilots inserted among data subcarriers outperforms the LS estimator and the STA estimator. The OFDM UAC simulator also includes the MIMO system. It is found that the MIMO technique could improve both the transmission rate and reliability of OFDM UAC. Therefore, it is suggested to include the specifications of MIMO transmission in the future OFDM UAC standard.

ACKNOWLEDGMENT

We would like to thank the Institute of Electrical and Electronics Engineers (IEEE) for accepting our proposal and funding our research.

REFERENCES

[1] John Heidemann, Wei Ye, Jack Wills, Affan Syed, and Yuan Li. Research challenges and applications for underwater sensor networking. In *Proceedings of Wireless Communications and Networking Conference*, pages 228–235, Las Vegas, NV, April 3-26, 2006.

[2] Ian F. Akyildiz, Dario Pompili, and Tommaso Melodia. Underwater acoustic sensor networks: Research challenges. *Elsevier Ad Hoc Networks Journal*, 3(3):257–279, March 2005.

[3] Mandar Chitre, Shiraz Shahabudeen, and Milica Stojanovic. Underwater acoustic communications and networking: Recent advances and future challenges. *Marine Technology Society Journal*, 42(1):103–116, Spring 2008.

[4] Roald Otnes, Trond Jenserud, Jan E. Voldhaug, and Connie Soldberg. A roadmap to ubiquitous underwater acoustic communications and networking. In *Proc. Underwater Acoustic Measurement: Technologies and Results*, pages 1–8, Nafplion, Crete, Greece, 2009.

[5] Lee Freitag and Sandipa Singh. Multi-user frequency hopping underwater acoustic communication protocol. *Woods Hole Oceanographic Institution, Technical Report*, 2000.

[6] Lee Freitag, Matthew Grund, Sandipa Singh, James Partan, Peter Koski, and Keenan Ball. The WHOI micro-modem: an acoustic communications and navigation system for multiple platforms. In *Proceedings of MTS/IEEE Oceans Conference*, pages 1086–1092, Washington, DC, September 17-23, 2005.

[7] Baosheng Li, Shengli Zhou, Milica Stojanovic, Lee Freitag, and Peter Willett. Multicarrier communication over underwater acoustic channels with nonuniform Doppler shifts. *IEEE Journal of Oceanic Engineering*, 33(2):198–209, April 2008.

[8] Milica Stojanovic. OFDM for underwater acoustic communications: Adaptive synchronization and sparse channel estimation. In *Proceeding of International Conference on Acoustics, Speech and Signal Processing*, pages 5288–5291, Las Vegas, NV, March 30-April 4, 2008.

[9] LAN/MAN Standards Committee of the IEEE Computer Society. 802.11p-2010 IEEE standard for information technology-local and metropolitan area networks-specific requirements-part 11: Wireless LAN medium access control (MAC) and physical layer (PHY) specifications amendment 6: Wireless access in vehicular environments. *URL: http://standards.ieee.org/findstds/standard/802.11p-2010.html*.

[10] LAN/MAN Standards Committee of the IEEE Computer Society. 802.11a-1999 IEEE Standard for Telecommunications and Information Exchange Between Systems-LAN/MAN Specific Requirements-Part 11: Wireless Medium Access Control (MAC) and physical layer (PHY) specifications: High Speed Physical Layer in the 5 GHz band. *URL: https://standards.ieee.org/findstds/standard/802.11a-1999.html*.

[11] Mehmet K. Ozdemir and Huseyin Arslan. Channel estimation for wireless OFDM systems. *IEEE Surveys and Tutorials*, 9(2):18–48, July 2007.

[12] Joseph A. Fernandez, Kevin Borries, Lin Cheng, B. V. K. Vijaya Kumar, Daniel D. Stancil, and Fan Bai. Performance of the 802.11p physical layer in vehicle-to-vehicle environments. *IEEE Transactions on Vehicular Technology*, 61(1):3–14, January 2012.

[13] Milica Stojanovic and James Preisig. Underwater acoustic communication channels: Propagation models and statistical characterization. *IEEE Communications Magazine*, 47(1):84–89, January 2009.

[14] Parastoo Qarabaqi and Milica Stojanovic. Acoustic channel simulator. *Available in http://oalib.hlsresearch.com/Rays*, 2014.

[15] Parastoo Qarabaqi and Milica Stojanovic. Statistical characterization and computationally efficient modeling of a class of underwater acoustic communication channels. *IEEE Journal of Oceanic Engineering*, 38(4):701–717, October 2013.

[16] Peter W. Wolniansky, Gerard J. Foschini, G. D. Golden, and Reinaldo A. Valenzuela. V-BLAST: An architecture for realizing very high data rates over the rich-scattering wireless channel. In *URSI International Symposium on Signals, Systems, and Electronics*, pages 295–300, Pisa, September 29-October 2, 1998.